$O(^1S \rightarrow {}^1D,{}^3P)$ branching ratio as measured in the terrestrial nightglow

T. G. Slanger,[1] P. C. Cosby,[1] B. D. Sharpee,[1] K. R. Minschwaner,[2] and D. E. Siskind[3]

Received 13 July 2006; revised 14 August 2006; accepted 13 September 2006; published 30 December 2006.

[1] The branching ratio of the two optically forbidden atmospheric emission lines, $O(^1S - {}^1D)$ at 557.7 nm and $O(^1S - {}^3P)$ at 297.2 nm, is a fixed number in the upper atmosphere because the $O(^1S)$ level is common to both lines. The value for the ratio A(557.7)/A(297.2) currently recommended by NIST is 16.7, and the ratio found in the laboratory is somewhat larger. Field observations require space-based instruments, in which case calibration between the two wavelength regions is the critical issue. We circumvent this problem by using the O_2(*A-X*) Herzberg I emission system as a bridge between the UV region below 310 nm and the ground-accessible region above that wavelength. These two spectral regions can be separately calibrated in terms of intensity, and the results of a disparate set of observations (satellite, rocket, ground-based sky spectra) lead to a quite consistent value of 9.8 ± 1.0 for A(557.7)/A(297.2). This conclusion has consequences for auroral and dayglow processes and for spectral calibration. It is particularly important to ascertain the cause of the substantial difference between this value and those from theory.

Citation: Slanger, T. G., P. C. Cosby, B. D. Sharpee, K. R. Minschwaner, and D. E. Siskind (2006), $O(^1S \rightarrow {}^1D,{}^3P)$ branching ratio as measured in the terrestrial nightglow, *J. Geophys. Res.*, *111*, A12318, doi:10.1029/2006JA011972.

1. Introduction

[2] The oxygen 557.7 nm green line is the earliest recognized feature of the visible nightglow [*Ångstrom*, 1869], while the 297.2 nm line is one of the more prominent components of the UV nightglow. As these two lines originate on the same $O(^1S)$ level, their intensity ratio is fixed. Nevertheless, between theoretical, laboratory, and atmospheric determinations, there is still poor agreement on the value of the ratio.

[3] In Table 1 we list the results of theoretical calculations and laboratory measurements over the years. Because of the relative stability of the theoretical values, the ratio of 16 has generally been adopted for the intensity ratio I(557.7)/I(297.2), defined here as $\mathcal{R}$.

[4] However, there are UV dayglow and visible auroral measurements that suggest that a value of 16 leads to certain discrepancies, and so there has continued to be a level of uncertainty about the ratio. Sharp and Siskind pointed out a number of years ago that their results from rocket observations of the UV nightglow were incompatible with the high values for the transition probability ratio shown in Table 1 [*Sharp and Siskind*, 1989].

[5] Their conclusions were based on the idea of using the O_2 *A-X* Herzberg I (Hz I) state distribution as a bridge linking the two wavelength regions because considerable work had already been done from ground-based measurements to establish the intensity relationship between the 557.7 nm line and the Herzberg I bands. In their rocket study they were able to characterize the relationship between the 297.2 nm line and the heart of the Herzberg I distribution, the emission below 300 nm, concluding that the intensity ratio between the total Herzberg I distribution and the 297.2 nm $O(^1S)$ line has a value of 18. Combined with the fact that there is general agreement that the ratio between the total Herzberg I distribution and the 557.7 nm $O(^1S)$ line is close to 2 immediately leads to $\mathcal{R} = 9$. It is the discrepancy between this value and those given in Table 1 that we set out to explore.

[6] We believe that the recent use of well-calibrated sky spectra from large telescopes [*Cosby et al.*, 2006; *Hanuschik*, 2003], combined with repeated UV nightglow observations from rockets and satellites [*Hennes*, 1966; *Minschwaner et al.*, 2004; *Owens et al.*, 1993; *Sharp and Siskind*, 1989], has led to our ability to assign a definitive value to $\mathcal{R}$. Other questions then surface because of the discordance of this value with theory and the even greater disagreement with laboratory results. We outline here the sources of information for our analysis:

[7] 1. The rocket experiment of *Hennes* [1966] was the first in which the dispersed Herzberg I band emission was viewed in the region below the ozone cutoff, and the spectrum covered the 260–385 nm region. The spectral resolution is not sufficient to resolve all bands, but it is adequate to show consistency with subsequent measurements.

[1] Molecular Physics Laboratory, SRI International, Menlo Park, California, USA.
[2] New Mexico Institute of Mining and Technology, Socorro, New Mexico, USA.
[3] Naval Research Laboratory, Washington, D.C., USA.

0148-0227/06/2006JA011972

Table 1. Theoretical, Laboratory, and Observational Determinations of $\mathcal{R}$ = I(557.7)/I(297.2)

Reference	Value
Theory	
[*Condon*, 1934]	11.1
[*Pasternack*, 1940]	24.4
[*Garstang*, 1951]	16.4
[*Yamanouchi and Horie*, 1952]	30.4
[*Garstang*, 1956]	17.6
[*Fischer and Saha*, 1983]	13.6
[*Baluja and Zeippen*, 1988]	13.0
[*Galavis et al.*, 1997]	14.2
[*Fischer and Tachiev*, 2004]	16.1
Current NIST recommendation[a]	16.7
Laboratory Experiments	
[*LeBlanc et al.*, 1966]	22 ± 2
[*McConkey et al.*, 1966]	18.6 ± 3.7
[*Kernahan and Pang*, 1975]	23.7 ± 2.4
Nightglow	
Deduced from *Sharp and Siskind* [1989]	~9
[*Torr et al.*, 1993]	24 ± 2
Broadfoot (private communication, 2006), from 1994 Arizona GLO observations	8.2 ± 0.8
Present results	9.8 ± 1.0

[a]Available at http://physics.nist.gov/cgi-bin/AtData, taken from *Wiese et al.* [1996].

[8] 2. In a later rocket study [*Sharp and Siskind*, 1989], the region below 300 nm was viewed with improved resolution, with the 297.2 nm OI line being cleanly resolved from the neighboring Herzberg I 5-3 band. It was pointed out that a significantly lower value for $\mathcal{R}$ was needed to fit the observations than the one in use at the time.

[9] 3. In a ground-based study [*Stegman and Murtagh*, 1991] the Herzberg I to 557.7 nm ratio was determined based on higher-resolution measurements than previously available. The analysis of many spectra produced a robust value for the ratio, but an apparent anomaly was discovered for the v = 5 level of the $O_2(A)$ state. The present analysis clarifies this issue.

[10] 4. Many spectra of the 250–300 nm region were collected on the ISO/ATLAS-1 mission, with good spectral resolution [*Owens et al.*, 1993], and we have analyzed 38 of them. All these data suffer from the flaw that the given tangent ray heights are unrealistic, but this is not an impediment to our analysis, as will be discussed. On the same mission a value for $\mathcal{R}$ was determined, from simultaneous 297.2 and 557.7 nm measurements [*Torr et al.*, 1993], but the value disagrees with the ultimate results of our analysis.

[11] 5. Observations from the ISAAC spectrometer on the ARGOS satellite [*Wolfram et al.*, 1999] viewed the 250–300 nm region, with similar spectral resolution to the earlier data sets [*Owens et al.*, 1993; *Sharp and Siskind*, 1989]. Many scans are available at different altitudes, and for the purposes of this study, we view the 260–300 nm region.

[12] 6. The use of astronomical sky spectra makes it possible to measure the terrestrial nightglow with high precision down to the ozone cutoff [*Slanger et al.*, 2004a; *Slanger et al.*, 2001b]. In this manner, it is possible to use very detailed spectral information to reevaluate the ratio of Herzberg I to 557.7 nm emission, and the value generally in use was confirmed.

[13] In contrast to the range of values encountered for the O(^{1}S) branching ratio shown in Table 1, the two lines associated with the emission from O(^{1}D) at 630.0 and 636.4 nm show close agreement between atmospheric observations and theory [*Sharpee and Slanger*, 2006]. The I(630.0 nm)/I(636.4 nm) is equal to 2.997 ± 0.016 and can be compared to the ratio of 2.997 determined by *Storey and Zeippen* [2000] in a recent set of calculations. The same calculation procedure gives a value of 14.2 for the O(^{1}S) case [*Galavis et al.*, 1997], this value being somewhat lower than most theoretical determinations (Table 1).

[14] A further example of the agreement of theory with atmospheric observations arises in the case of the N(^{2}D–^{4}S) line pair at 519.8 and 520.0 nm. In this instance, there are two emitting levels in the N(^{2}D) state, so the line intensity ratio is not forced to be fixed, as is true for the O(^{1}D) and O(^{1}S) states. Nevertheless, the two N(^{2}D) levels are collisionally equilibrated in the atmosphere, and a precisely constant ratio between the intensities of the two lines from Keck I/HIRES and Keck II/ESI data is determined [*Sharpee et al.*, 2005]. The value is 1.759 ± 0.014 for I(519.8 nm)/I(520.0 nm) and that obtained from the most recent Breit-Pauli calculation is 1.788 [*Fischer and Tachiev*, 2004]. However, a range of values from earlier calculations can be found in the literature, and the present NIST evaluation recommends 2.41 [*Wiese et al.*, 1996].

[15] It is evident that a basic difference between the O(^{1}D–^{3}P) and N(^{2}D–^{4}S) cases on the one hand and the O(^{1}S–^{1}D,^{3}P) case on the other is the fact that the wavelength difference between the two lines in the first two instances is 6.4 and 0.2 nm, respectively, while it is 260 nm for O(^{1}S). Intensity calibration is therefore of primary concern for any study of the 557.7/297.2 branching ratio.

2. Results

2.1. Herzberg I Bridge

[16] The fact that one half of the Herzberg I emission bands can be observed from the ground and the other half can be seen from space, below 300 nm, suggests a way to determine the intensity ratio of the O(^{1}S) emission lines. Simultaneous space-based atmospheric measurements of emission in the two spectral regions in question are rare. Even if accomplished, characterizing the differences in instrumental sensitivities to develop a reliable intensity calibration across such a wide breadth of wavelength is difficult and subject to uncertainty. Nevertheless, two such measurements are discussed below [*Broadfoot et al.*, 1997; *Torr et al.*, 1993]. As we will show, the Herzberg I distribution of photons from these emissions can be fully characterized, allowing one to relate the 297.2 and 557.7 nm line intensities in a meaningful way. Thus it is possible to deal with the UV and visible portions of the nightglow separately, which is in any case necessary because much of the UV data only extend as far as 300 nm, while the ground-based data are limited by the ozone cutoff near 310 nm.

[17] To use the Herzberg I emission for this purpose, two things are required: that the pattern of bands, i.e., the vibrational distribution, is fixed and that the transition probabilities for the matrix of bands be known, at least in relative terms. The vibrational distribution for the Herzberg I system has been investigated numerous times,

Table 2. Measurements of Nightglow Intensities in Visible Region

Source	I(Herzberg I)	I(557.7)	Ratio
Photometer Measurements			
[*Thomas et al.*, 1979]			5–7
[*Thomas and Young*, 1981]	600–700 R	90 R	6.6–7.8
[*Murtagh et al.*, 1986]	230	121	1.9
	302	142	2.1
	370	165	2.2
[*Ogawa et al.*, 1987]	465	180	2.6
[*Stegman and Murtagh*, 1988]			2.5–3.0
[*Stegman and Murtagh*, 1991]	0–600	0–300	2.0–2.5
[*Melo et al.*, 1997]	167	135	1.24
Spectrometer Measurements (Deduced From 297.2 nm Intensity)			
[*Sharp and Siskind*, 1989]	1400	1800	0.78
[*Hennes*, 1966]	(reanalysis by Sharp and Siskind)		1.0

most recently with sky spectra from the Keck I telescope and the HIRES echelle spectrograph [*Slanger et al.*, 2004a], and the distribution is now well known and essentially invariant. The transition probabilities are well approximated by the product of the Franck-Condon factor and the cube of the transition frequency, and we will show here that this is true in both spectral regions.

[18] The determination of the ratio of the intensities of the Herzberg I emission to the green line has been previously evaluated [*Sharp and Siskind*, 1989], and in Table 2 we show a series of results obtained over the years, adapted from Table 3 of Sharp and Siskind. These evaluations typically show a value for the ratio of the total Herzberg I intensity to that of the green line of 2.0–2.5 for the photometer measurements. The two values measured by photometer that are anomalously high are unlikely to be correct and would in any case lead to unrealistically low values for $\mathcal{R}$. For the two rocket-based spectrometer results, the values are low because their 297.2 nm measurements were converted to 557.7 nm intensities by using the value for $\mathcal{R}$ of Kernahan and Pang (Table 1). As we will show, it seems that the true value of $\mathcal{R}$ is smaller by a factor of about 2.5, which has the effect of raising the I(Hz I)/I(557.7 nm) ratios by the same factor, thus bringing the data into line with the values from direct 557.7 nm detection. As pointed out by Sharp and Siskind, their deduced 557.7 nm intensity of 1800 Rayleighs (R) is unprecedentedly high, which led them to suspect that the high experimental values of $\mathcal{R}$ could not be correct. To proceed in our analysis, we present data on the six studies described in section 1.

2.2. *Hennes* [1966]

[19] The first atmospheric observation of the resolved Herzberg I bands below 300 nm was carried out from a rocket [*Hennes*, 1966]. The wavelength range covered was unusually broad, including emission from 260 to 385 nm, which encompasses 90% of the Herzberg I emission. The system was intensity calibrated, and absolute intensities were provided for specific wavelength intervals. Subsequently, an attempt was made to assign individual band intensities, which was somewhat problematic because the resolution was not high enough to accurately deduce a vibrational distribution and because the Chamberlain bands could not be properly taken into account. The particular virtue of Hennes' spectrum is that it provides a link between ground-based spectra, which are cut off near 310 nm, and the UV rocket/satellite data, which usually do not extend beyond 300 nm.

[20] For our purposes the key is to determine a value for the 297.2 nm line intensity with respect to the nearby Herzberg I bands. This can easily be done from Hennes' spectrum, although the author went astray when he chose to deduce the line intensity not from his own data but from an approximately simultaneous ground-based measurement of the 557.7 nm line intensity and application of the supposedly known value for $\mathcal{R}$ of 16. As a result, his estimation of intensities for the 297.2 nm line and the nearby Herzberg I 5-3 band is clearly at odds with his spectrum. From the latter we can determine from simple modeling that the Herzberg I 5-3 to 297.2 nm intensity ratio is 0.8, whereas Hennes' analysis gives a value of 3.

[21] Because Hennes covered such a wide range of Herzberg I bands, we are able to obtain an approximate value for the intensity ratio of the entire Herzberg I system to the 297.2 nm line intensity, using our own analysis for the latter. Hennes' total computed 260–385 nm emission intensity is 600 R, and this spectral region contains 90% of the Herzberg I emission. The Chamberlain band emission is also strong, and the largest fraction is found in the 300–385 nm region. The ratio of Herzberg I to Chamberlain emission is estimated as 4 [*Slanger and Huestis*, 1983], leading to the conclusion that the total Herzberg I emission is about 530 R. Hennes reported that the total Hz I 5-3 band + 297.2 line intensities amounted to 46 R, and from our modeling of the band shape, we find that the 297.2 nm emission is 26 R of this sum. We thereby conclude that the I(ΣHz I)/I(297.2 nm) ratio is 530/26 = 20, and although our reconstruction of the data is not very accurate, this figure is in complete accord with the numbers to be derived below.

Table 3. Comparison of Strong Herzberg I Bands Between UVES Data and Calculations Based on the Known Distribution and the $q\nu^3$ Product With Normalization to the 4-4 Band[a]

Herzberg I Band	UVES Intensity	Intensity From $q\nu^3$ and Population Distribution	I[UVES] I[$N(v')q\nu^3$]	r-centroid
4-4	25 R	25 R	1.00	1.3773
3-4	15.6	17.9	0.87	1.3854
7-6	12.9	10.3	1.25	1.3910
4-5	15.8	13.2	1.20	1.3926
2-4	7.0	7.6	0.92	1.3939
6-6	8.9	6.9	1.29	1.3988
3-5	16.4	16.5	0.99	1.4015
2-5	7.5	10.4	0.72	1.4107
6-7	11.6	10.9	1.06	1.4130
5-7	9.9	10.4	0.95	1.4217
2-6	7.3	8.9	0.82	1.4277
5-8	9.3	8.6	1.08	1.4369
4-8	9.5	9.9	0.96	1.4471
1-7	6.7	6.5	1.03	1.4563
6-10	6.1	7.2	0.85	1.4674
3-9	5.7	7.0	0.81	1.4752
Sum	175 R	168 R (26% of total)		

[a]Ordering is in terms of the r-centroid.

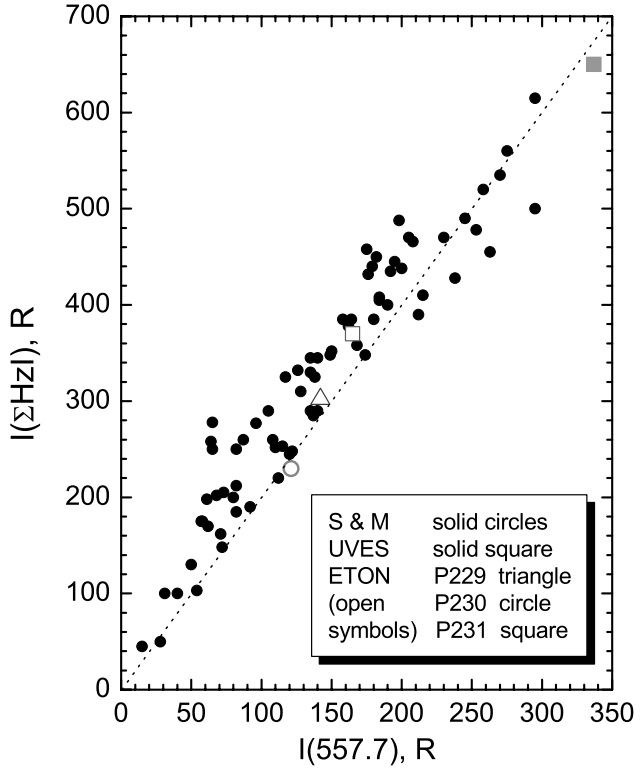

Figure 1. Plot of the total observed O_2 *A-X* Herzberg I to 557.7 nm intensities (adapted from *Stegman and Murtagh* [1991, Figure 4]), the dashed line having a slope of 2. The ratio determined from VLT/UVES spectra is shown as the single solid point at (337 R, 650 R). The results of measurements from the ETON campaign are also shown on the plot.

2.3. *Sharp and Siskind* [1989]

[22] These authors flew a spectrometer on a rocket and observed the 260–300 nm region [*Sharp and Siskind*, 1989]. The Herzberg I bands and the 297.2 nm line were well resolved, and with reasonable assumptions concerning the vibrational distribution and transition probabilities for the band system, an intensity ratio of 18 was deduced for the total Herzberg I system to the 297.2 nm line, in close agreement with the conclusions from Hennes' data. Note that the Chamberlain bands are absent below 300 nm, and the contributions from the Herzberg II and III bands are small. If these contributions are approximated and subtracted, the ultimate effect on $\mathcal{R}$ will be to make it smaller by about 15%.

2.4. *Stegman and Murtagh* [1991]

[23] This is a ground-based study of the nightglow over a broad spectral region and down to the UV ozone cutoff [*Stegman and Murtagh*, 1991]. The data are of sufficiently high resolution that in conjunction with modeling of the emission, it is possible to determine the Herzberg I intensity separately from the Chamberlain bands.

[24] Of direct interest here is the plot that was generated of the intensity ratio of the total Herzberg I emission to the oxygen green line, their Figure 4 adapted here as Figure 1. As seen in the figure, the measured ratios scatter about a line with a slope of two at higher overall intensities and about a line with a somewhat higher slope at lower overall intensities. The single solid point near the highest measured intensities is from the UVES/VLT data that is described below. It should be noted that only a slope considerably less than two can be compatible with the high values of $\mathcal{R}$ reported in theoretical calculations or laboratory determinations (Table 1). Also shown in Figure 1 are the data obtained from the multirocket ETON campaign [*Murtagh et al.*, 1986], where three separate flights show a value for I(ΣHzI)/I(557.7) close to 2.0.

[25] Because it is convenient to measure and model the Herzberg I 5–3 band and the 297.2 nm together, it is important to establish the intensity ratio of the Herzberg I 5–3 band to the total Herzberg I intensity. From the matrix of bands determined by Stegman and Murtagh, this fraction is 0.035. However, this value is based on their own derived vibrational distribution for the A(v) levels, for which they reported that the v = 5 emission was anomalously low. This observation is not confirmed by any other work and is discussed in the most recent measurement of this distribution [*Slanger et al.*, 2004a], where it was suggested that the lack of strong v = 5 vibrational bands observable from the ground is responsible for this discrepancy.

[26] The predicted relative intensities of the 5-3 band and the neighboring 6-3 band are 35.4 R and 53.9 R per 1000 R of Herzberg I emission in the Stegman and Murtagh matrix. Instead, published UV spectra show these two bands to be very close to equal in intensity [*Owens et al.*, 1993; *Sharp and Siskind*, 1989], and this is also evident from the ISAAC spectra, shown later. In the matrix of bands calculated below from the recent vibrational distribution [*Slanger et al.*, 2004a], the intensities of the two bands are within 5% of each other, and the 5-3 fraction of the total Herzberg I system is 0.044. This is the number we use to convert measured I(Hz I 5-3)/I(297.2 nm) ratios to [ΣHzI]/[297.2]. Any higher value will reduce the ultimate derived value of $\mathcal{R}$, and in the matrix given by *Degen* [1977], a value of 0.053 is quoted. This appears to be the result of a somewhat skewed vibrational distribution, where the A(v = 4) level is the one most populated, rather than the v = 6 level [*Slanger et al.*, 2004a].

[27] Transition probabilities have been calculated for the Herzberg I system by *Bates* [1989], and in that compilation the A-factors for the 5-3 and 6-3 bands are equal. As the A(v = 5,6) populations used in the present analysis are essentially equal, the same should be true of the 5-3 and 6-3 intensities from any atmospheric source. This is indeed the case, supporting our choice of the I(5-3)/I(ΣHzI) value of 0.044.

2.5. ISO ATLAS-1 Mission

[28] There is considerable data available from the ISO/ATLAS mission [*Owens et al.*, 1993], where the airglow was measured over the 276–300 nm region with multiple spectrometers. A serious problem with the data analysis is that the tangent ray heights (TRH) that were determined for the mesospheric emissions were much too low, and this has raised questions about the use of the data, but we believe that for our needs this is not really an impediment. It seems that a value of 17 km added to the stated TRH is a reasonable approximation to the true altitude, as concluded

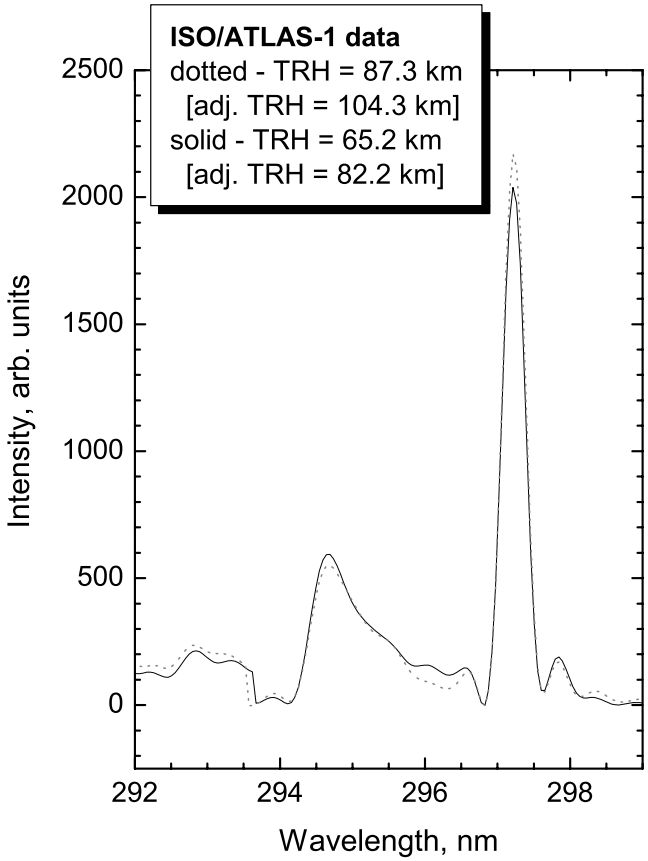

Figure 2. Representative data from ISO showing high and low tangent ray height spectra in the vicinity of the Herzberg I 5-3 band and the 297.2 nm line.

from the superposition of the 297.2 nm and Herzberg I data with altitude profiles from the ETON data set [*Greer et al.*, 1986].

[29] We focus on the 290–300 nm region, i.e., the location of the Herzberg I 5–3 band and the 297.2 nm line. Figure 2 shows a representative portion of the data, for high and low altitude, demonstrating that the quality and resolution is comparable to that of the Sharp and Siskind study [*Sharp and Siskind*, 1989]. We have used 32 data sets from the ISO investigation, covering the adjusted 82–109 km altitude range. From these, the areas of the 5-3 band and the 297.2 nm line are integrated, and plotted in Figure 3. We find the I(5-3)/I(297.2) ratio to be 0.86 ± 0.03 (1 − σ), comparable to that obtained earlier [*Hennes*, 1966; *Sharp and Siskind*, 1989], as well as the data from the ISAAC/ARGOS mission described in the next section.

[30] The linear relationship between the 5-3 and 297.2 nm intensities is consistent with that found by Stegman and Murtagh for I(ΣHzI)/I(557.7), an indication that the 5-3 band always comprises the same fraction of the total Herzberg I system. Clearly, knowing this fraction leads from these two data sets to a value for $\mathcal{R}$. We note that except for intensity, these spectra do not change with tangent ray height. This is an indication that ozone absorption plays no role at the altitudes investigated, because ozone absorption cross sections change rapidly between 276 and 300 nm, which would lead to a depletion of signal at shorter wavelengths if its absorption were significant.

2.6. UV/Visible Space Shuttle Measurements

[31] There are two sets of measurements that have been reported covering the UV/visible region and encompassing both O(^{1}S) lines [*Torr et al.*, 1993; *Broadfoot et al.*, 1997]. They are both dayglow observations, but this should not be relevant in terms of the value of $\mathcal{R}$ retrieved. Data taken from the MSX satellite exist, but a calibrated spectrum has not yet been published.

[32] The measurements by *Torr et al.* [1993] explicitly give altitude profiles for the 297.2 and 557.7 nm volume emission rates, and the ratio we obtain from these data has a value of 24 ± 2, independent of altitude from 110 to 270 km. The agreement with the laboratory investigations is very good, less good with theory, and poor with the value of 9.8 ± 1 that we propose. There is little information given regarding intensity calibration.

[33] The dayglow data from the Arizona GLO experiment do not contain a specific determination of the two line intensities, but these have been provided to us (A. L. Broadfoot, private communication, 2006). The limb intensities, for a tangent ray height of 175 ± 5 km, are 9405 R for the 557.7 nm line and 1149 R for the 297.2 nm line, leading to a ratio of 8.2 ± 0.8. The data come from different spectrographs, and the overall intensity calibration is carried out with the use of star spectra. This is by far the lowest ratio measured and is in good accord with the value reported here. The fact that two equivalent determinations [*Torr et al.*, 1993; *Broadfoot et al.*, 1997] give values of

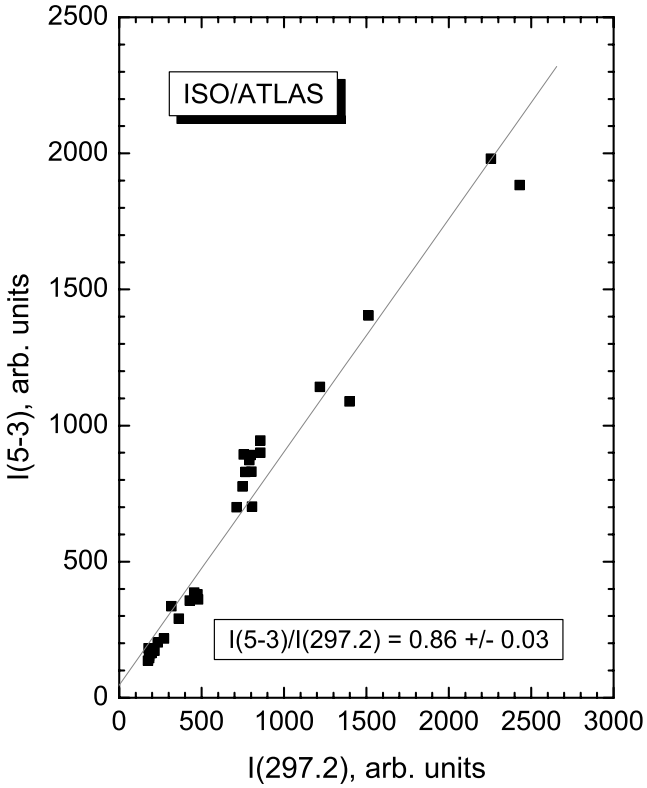

Figure 3. Plot of I(Hz I 5-3) versus I(297.2 nm) from ISO data.

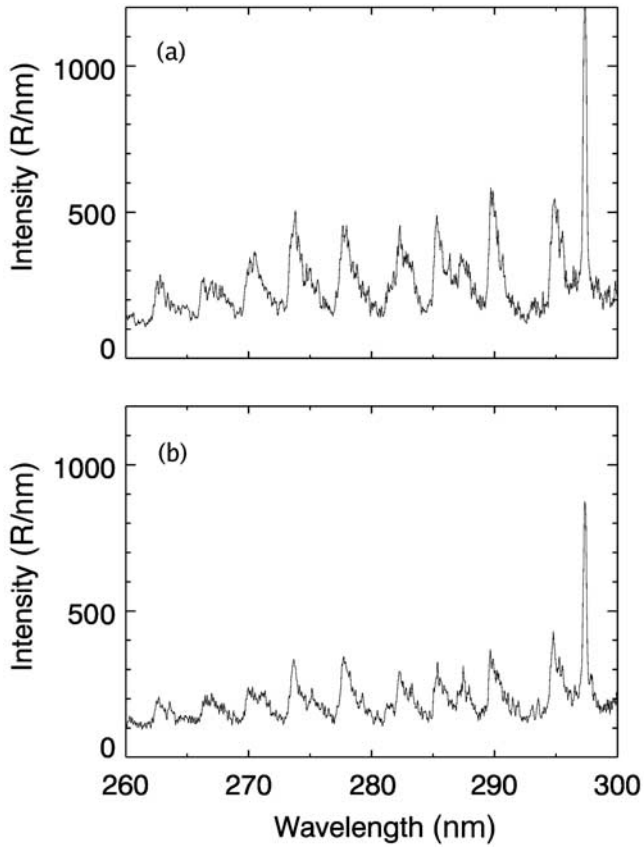

Figure 4. Nightglow spectra observed by ISAAC at two tangent ray heights: (a) 97 km, (b) 81 km. Both spectra are averages of limb scans over the latitude range 20°S to 20°N obtained on 23 November 1999.

$\mathcal{R}$ differing by a factor of three points to intensity calibration being the most likely cause.

2.7. ISAAC/ARGOS Data

[34] There is a wealth of data from the ISAAC spectrometer on the ARGOS spacecraft in the 260–301 nm region, with unambiguous tangent ray height determination. We present these data in several figures.

[35] Figure 4 shows the 260–300 nm spectral region at two different tangent ray heights. In terms of spectral distribution they are essentially identical, in agreement with the ISO/ATLAS-1 results. This reinforces an important conclusion, that the Herzberg I distribution viewed from the ground is not averaged over altitudes but represents a single distribution. This was shown by the ETON results, where the conclusion was reached that the $O_2(A)$ vibrational distribution is not altitude-dependent [*Murtagh et al.*, 1986]. In Figure 5 are presented determinations of the same parameter as shown in Figure 3, the I(5-3)/I(297.2) ratio as a function of altitude (instead of tangent ray height). Agreement with the ISO/ATLAS-1 data is quite good, showing the constancy of the ratio with altitude. Carrying the analysis a step further, in Figure 6, the areas of the HzI bands below 300 nm and the 297.2 nm line are determined for several spectra, and the I(ΣHzI)/I(297.2) ratio is plotted as a function of altitude, making the approximation that the Herzberg bands below 300 nm represent 40% of the total

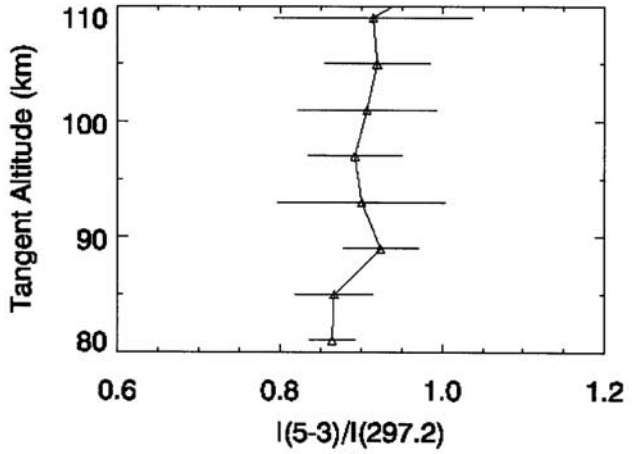

Figure 5. ISAAC measured ratio of Herzberg I 5-3 band intensity to oxygen 297.2 nm line intensity as a function of altitude. Ratios are means over the time period 21–27 November 1999 and over the latitude range 20°S–40°N. Error bars denote one standard deviation of the data. The mean ratio from 80 to 105 km is 0.89 ± 0.03.

distribution. We see that from 80 to 105 km, where most of the Herzberg I and 297.2 nm emission originates, the ratio is invariant over all measured latitude ranges, with a value of 20.3 ± 3.1, in agreement with our analysis of Hennes' data. The ISO/ATLAS-1 results from Figure 3 also show the invariance of the equivalent I(5-3)/I(297.2 nm) ratio. Thus not only is the Herzberg I distribution fixed, the same is true for the ratio of Herzberg I to O(^{1}S) emission. This is in agreement with the ground-based determination of the I(HzI > 315 nm)/I(557.7 nm) ratio by Stegman and Murtagh

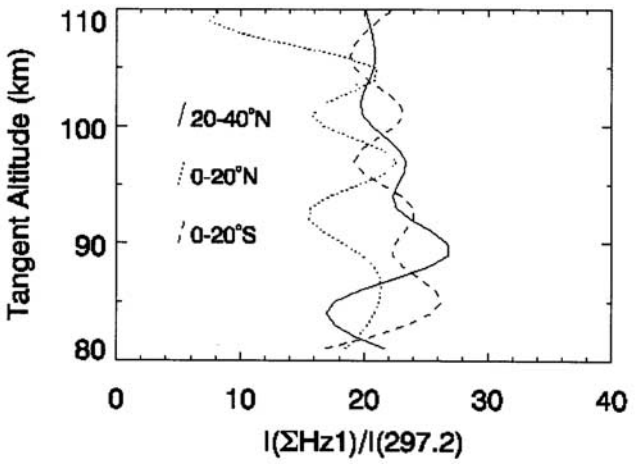

Figure 6. ISAAC measured ratio of total Herzberg I intensity to the oxygen 297.2 nm line intensity as a function of altitude for 23 November 1999. The total Herzberg I intensity is calculated assuming the measured Herzberg I intensity below 300 nm is 40% of the total band system intensity. Three latitude ranges are displayed: 20–40°N (solid), 0–20°N (dotted), and 0–20°S (dashed). Overall mean ratio at 80–105 km is 20.3 ± 3.1 (1 − σ).

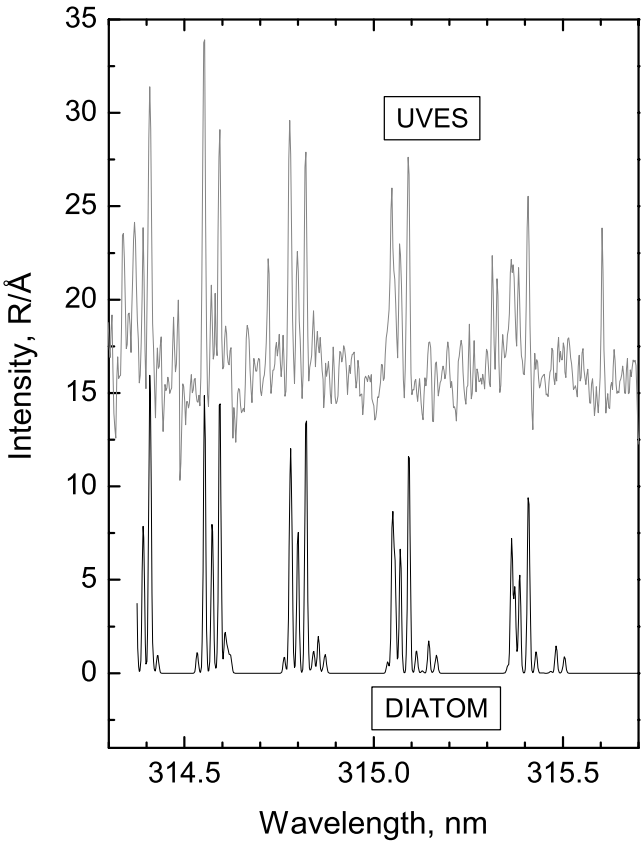

Figure 7. UVES/VLT spectrum of the Herzberg I 4-4 band [*Hanuschik*, 2003] and a DIATOM simulation of that band.

[*Stegman and Murtagh*, 1991] and with the ETON results [*Murtagh et al.*, 1986].

2.8. Astronomical Sky Spectra and the UVES/VLT Database

[36] Over the last several years, considerable use has been made of the sky spectra generated by astronomers to produce detailed pictures of the nature of weak atmospheric emissions. A sky spectrum is the blank sky telluric spectrum that astronomers produce in the course of their measurements to subtract from their object spectrum. These spectra are taken at high resolution with echelle spectrographs and have wide wavelength coverage and thus are most desirable for simultaneous observations of features in different wavelength regions [*Slanger and Copeland*, 2003; *Slanger et al.*, 2003a; *Slanger et al.*, 2003b; *Slanger et al.*, 2000a; *Slanger et al.*, 2004b; *Slanger and Osterbrock*, 2000]. The accuracy of the wavelength calibrations has been demonstrated [*Slanger et al.*, 2000b], and the spectra are calibrated in terms of intensity against standard stars.

[37] There are in total five band systems of O_2 that lie in the 250–500 nm region. In addition to the *A-X* Herzberg I transition, there are the A'-*a* Chamberlain bands, the *c-X* Herzberg II bands, the *c-b* bands [*Slanger et al.*, 2003b], and the A'-*X* Herzberg III bands. Of these, the Herzberg II and III bands will be strongest below 300 nm, the Chamberlain bands are most intense at 330–450 nm, while the *c-b* bands are most intense at 390–450 nm. In sky spectra above 310 nm [*Cosby et al.*, 2006; *Hanuschik*, 2003] the Chamberlain and *c-b* lines are fully resolved and present no interference. In the 260–385 nm rocket study of *Hennes* [1966], the unresolved Chamberlain bands should be taken into account, and in this region the Chamberlain bands have about 25% of the Herzberg I intensity.

[38] Sky spectra from the Ultraviolet Echelle Spectrograph (UVES) on the 8-m Kueyen component of the Very Large Telescope (VLT) in Paranal, Chile, have been compiled [*Hanuschik*, 2003] into an atlas of intensity-calibrated spectral lines, and the spectra themselves are available online. These spectra extend to the ozone cutoff in one direction and 1043 nm in the other and are proving to be a most useful tool for aeronomic research. Almost all of the 2810 listed lines have now been identified, and the O_2 and OH bands throughout the region can be accurately simulated [*Cosby et al.*, 2006]. Here, we use these data to evaluate the intensities of the Herzberg I bands, and with knowledge of the intensity distribution among all vibrational levels of the $O_2(A)$ state, we can then determine the intensity of the entire system. The green line is of course a prominent feature of the spectrum. The same technique was used in an earlier study [*Stegman and Murtagh*, 1991], but the resolution of the UVES spectra $-\lambda/\Delta\lambda$ = 45,000 is substantially greater.

[39] From data obtained with the HIRES echelle spectrograph on the Keck I telescope, Mauna Kea, Hawai'i, a vibrational distribution of the Herzberg I bands was obtained in spite of the fact that the spectra were not intensity-calibrated. This is possible because of the overlapping of bands in limited wavelength regions, from which a matrix can be built up. The resultant distribution was quite similar to that obtained in most other investigations, with the exception that more emission was seen from the $v' = 0$ level [*Slanger et al.*, 2004a], and there is no intensity anomaly at $A(v' = 5)$.

[40] From the determination of the vibrational distribution based on multiple bands from a given upper level, it was concluded that the intensities are proportional to the product of the Franck-Condon factor and the cube of the transition frequency, i.e., that the transition moment did not vary significantly with r-centroid. This is in accord with other studies [*Fateev et al.*, 1996] and with the set of transition probabilities calculated by *Bates* [1989]. It is therefore a simple matter to calculate the matrix of vibrational bands as done by others [*Degen*, 1972; *Stegman and Murtagh*, 1991]. In Table 3 we show the intensities of strong bands accessible to UVES, where we normalize to the 25 R measured intensity of the 4-4 band. Figure 7 shows a portion of the UVES spectrum of the 4–4 band, and a 200 K simulation from the DIATOM™ program. The baseline is far from smooth, and the spectrum contains extraneous emission lines and significant Fraunhofer absorption lines, but the nightglow and simulation fit reasonably well, and we have many bands to average over.

[41] We use the measured UVES intensities and compare them to the $N(v')q\nu^3$ product, $N(v')$ representing the vibrational distribution of the $O_2(A)$ state [*Slanger et al.*, 2004a]. Normalization is made to the intensity of the 4-4 band. Table 3 gives the measured intensities, the $N(v')q\nu^3$ product, and their ratio. The bands are ordered in terms of the value of their r-centroid, and one sees that there is no particular trend; the values of the ratio cluster around the normalized

Table 4. Modeled Intensities Normalized to 4-4 Band Intensity of 25 R[a]

	N	v″ = 1	2	3	4	5	6	7	8	9	10	11	Sum	Degen
v′ = 0	0.20					1.1	2.2	3.4	4.4	4.6	4	2.9	22.6	6.3
1	0.27			1	2.6	4.8	6.7	6.5	4.2	1.4	0	0.5	27.7	15
2	0.38		1.1	3.6	7.6	10.4	8.9	4	0.3	0.8	3.2	3.5	43.4	30
3	0.64	1	4.3	11.4	17.9	16.5	6.9	0	2.8	7.0	4.7	0	72.5	56
4	0.85	2.6	10.2	21.7	25.0	13.2	0.8	3.3	9.9	6.1	0	2.6	95.4	107
5	0.95	3.5	16.9	28.3	22.6	4.9	1.2	10.4	8.6	0.5	3	6.7	106.6	107
6	1.00	8	22.7	29.7	14.8	0	6.9	11.9	2.5	1.5	7.2	3.1	108.3	99
7	0.92	9.7	23.3	23.5	6.4	0.9	10.3	6.8	0	5.2	4.9	0	91	83
8	0.54	6.7	13.8	10.6	1.1	2.2	6	1.4	0.9	3.7	0	0.6	47	38
9	0.35	4.5	8	4.7		2.3	3	0	1.4	1.7		1	26.5	13
10	0.16	1.8	2.8	1.3		1.1	0.8		0.7	0.4		0.5	9.4	10
													650 R	564 R
													I(557.7) = 337 R	
													Hz1/557.7 = 1.93	

[a]Underlined intensities refer to bands unobservable from the ground. Modeled intensities are measured in Rayleighs.

ratio of 1.0. The ab initio dipole moment function for the *A-X* transition has been calculated, but it affects the model line intensities by less than 10% over the r-centroid range in Table 3 [*Klotz and Peyerimhoff*, 1986]. Thus it is reasonable to use only the $N(v')q\nu^3$ product to characterize the UV bands below the ozone cutoff.

[42] In Table 4 we show the full matrix of bands, normalized to the 4-4 band intensity of 25 R. The Herzberg I bands below 300 nm are underlined, because this is the limiting wavelength in the ISAAC and ISO spectra; the head of the 4-3 band lies at just this wavelength. The summed intensity of all bands out to $v'' = 11$ is 650 R, and the 557.7 nm green line intensity for the UVES data set is 337 R. The value of Σ(Herz I)/I(557.7) is therefore 1.93, close to the values determined from the earlier field measurements shown in Table 2. The summed intensities for the matrix developed by *Degen* [1977] is also shown in Table 4, with values normalized to $v' = 5$ in the two distributions. The intensity sum from the older distribution is 564 R, only 15% smaller than in the present analysis, and this seems to be primarily due to the fact that the low-v levels, v = 0–2, are underestimated in the earlier spectrum.

[43] In rocket and satellite measurements below 300 nm, interference by the Herzberg II and III bands must be considered, but in fact they are quite weak compared to the Herzberg I bands [*Santoro et al.*, 1994], where it was estimated that each of these systems contributes only 7–10% of the Herzberg I intensity below 300 nm. In the spectral fitting of *Sharp and Siskind* [1989], the Herzberg II intensity is assigned a value of 11% that of Herzberg I, and Herzberg III is 13%. However, both the 5-3 band and the 297.2 nm line are similarly affected by bands of the Herzberg II and III systems, so any adjustment should be only at the 5% level. We will not consider this contamination further, and only in the case of the Hennes data does another O_2 system present significant interference.

[44] The data in Table 4 are based on ground-based observations, and predict the relative intensities of the Herzberg I bands below 300 nm, which can only be seen from space. Using the ISAAC data we find excellent agreement between observation and prediction, the only discrepancies occurring for weak Herzberg I bands that are contaminated by Herzberg II bands. We can thus claim that data covering the entire O_2(*A-X*) manifold is consistent with the O_2(*A*) vibrational band matrix shown in Table 4.

3. Discussion

3.1. Terrestrial Observations

[45] In Table 5 we summarize the results of this investigation. We see that all data sets give consistent values for I(5-3)/I(297.2) and that conversion to I(ΣHzI)/I(297.2) gives consistent values near 19, shown by both the ISO/ATLAS-1 and the ISAAC data to be altitude- and latitude-independent. There is general agreement that I(ΣHzI)/I(557.7) is close to 2.0, and combining the UVES result of 1.93 with a value of 19 for I(ΣHzI)/I(297.2) then leads to a value for $\mathcal{R}$ of 9.8, a number considerably lower than theory predicts or is measured in laboratory experiments but in agreement with earlier analysis [*Sharp and Siskind*, 1989]. It is difficult to provide error limits, but we believe that ±10% is a reasonable estimation. It should be noted that most adjustments that have not been fully accounted for will decrease the value of $\mathcal{R}$. One of these is the contribution of the weak Herzberg II and Herzberg III bands below 300 nm, as mentioned earlier.

[46] Another issue is the possible contribution of thermospheric O(^{1}S) to the green line signal seen in ground-based measurements. O(^{1}S) is produced in the equatorial nightglow by two processes, O-atom recombination in the MLT region and O_2^+ dissociative recombination in the ionosphere, the atom recombination process is much the stronger.

[47] A limb-viewing measurement from space discriminates strongly against the high-altitude source if the MLT region is being imaged. From the ground, the 557.7 nm signal is the sum of emission from both altitude regions. If we wish to compare the 297.2 nm emission from space with the 557.7 nm emission from the ground, we should take account of this difference in viewing geometry.

[48] Laboratory measurements of product yields from the dissociative recombination of O_2^+ show that the O(^{1}S) yield is 4% that of O(^{1}D) [*Petrignani et al.*, 2005]. The UVES/VLT nightglow atlas indicates that the red line(s) and green line had similar intensities for the given coaveraged sample. It follows that for these conditions, the *F* region green line makes only a 4% contribution to observation of the green line from the ground, and this percentage should then be subtracted from the deduced value for $\mathcal{R}$.

Table 5. Historical Summary of Analysis of $\mathcal{R}$

Data Source	I(5-3)/I(297.2)	I(ΣHzI)/I(297.2)	I(ΣHzI)/I(557.7)	$\mathcal{R}$
Hennes [1966]	0.8	20		
Sharp and Siskind [1989]		18		
Stegman and Murtagh [1990]			2.0–2.5	
ISO/ATLAS-1	0.86 ± 0.03	21 ± 3		
ISAAC/ARGOS	0.89 ± 0.03 (80–105 km)	20.3 ± 3.1		
UVES			1.93	
Current Analysis				9.8 ± 1.0

[49] However, the thermospheric green line contribution is not always small, and measurements of the green line from WINDII on UARS (G. Shepherd, private communication, 2006) show that at solar maximum conditions over both Hawai'i (Keck) and Northern Chile (VLT), the *F* region green line peak intensity can be on the order of 8% of that from the mesosphere. Integrating over altitude indicates that for such a situation the *F* region green line seen from the ground would be 25% of the total measured intensity. To isolate the mesospheric fraction, it is probably best to measure the 630.0 + 636.4 nm red line intensity and apply the factor of 0.04 to approximate the *F* region green line.

[50] It is important to recognize that the calculations themselves are not in good accord, as shown in Table 1. This is in marked contrast to the calculations for the O(^{1}D − ^{3}P) lines at 630.0 and 636.4 nm, where analogously to the O(^{1}S − ^{1}D,^{3}P) case, there is a single emitting level. It is significant that for the O(^{1}D) emissions, the lower levels are fine-structure levels of the same ground electron configuration terms ($^3P_{0,1,2}$), whereas for the O(^{1}S) emissions, the lower levels belong to different terms, $^3P_2$ and $^1D_2$ for 297.2 and 557.7 nm, respectively. In any case, theoretical agreement is not good for the value of $\mathcal{R}$, so it is a weak argument to claim that the preponderance of evidence favors values higher than our new value.

[51] The results of the laboratory studies (Table 1) are inconsistent with most of the atmospherically derived and the theoretical determinations. We cannot point out an experimental flaw, since agreement between the three studies is reasonable. The most obvious issues are wavelength calibration and pressure-induced emission. It has long been known that the 557.7 nm line is pressure-sensitive [*Black et al.*, 1975], whereas the 297.2 nm line is not [*Cunningham and Clark*, 1974], leading to an overestimation of $\mathcal{R}$ if the pressure is too high. In each of the three laboratory experiments, tests were applied to show that for the given conditions, the green line intensity did not increase with pressure. Accurate intensity calibration is difficult over as large a wavelength range as here required, and we feel that this is the most likely source of error.

[52] It is evident that if aeronomers attempt to combine data sets from space-based measurements of the 297.2 nm line with ground-based or space-based measurements using the green line, inconsistencies will appear if an incorrect value for $\mathcal{R}$ is applied. Just such a problem has arisen in studies of the O(^{1}S) yield from the reaction between $N_2(A^3\Sigma_u^+)$ and O(^{3}P) [*Hill et al.*, 2000]. From dayglow observations of the 297.2 nm line, the derived yield is about twice as large as what is found from auroral studies using 557.7 nm emission. Included in the calculations is a value for $\mathcal{R}$ of 24, from the work of *Kernahan and Pang* [1975]. Substituting a value of $\mathcal{R} \sim 10$ brings the dayglow and auroral values for the O(^{1}S) yield into much better agreement (S. C. Solomon, private communication, 2005).

[53] With reference to the calculations, we note that there is general agreement that the radiative lifetime of O(^{1}S) is close to 0.8 s [*Baluja and Zeippen*, 1988; *Fischer and Tachiev*, 2004; *Nicolaides et al.*, 1971], and of course 90–95% of the transition probability is associated with the O(^{1}S − ^{1}D) emission. It follows that the A-factor for this transition is known fairly precisely, so any calculation of $\mathcal{R}$ compatible with the value proposed here will require a significant increase in the O(^{1}S − ^{3}P) transition probability. The inclusion of higher-order terms in the magnetic dipole operator expansion [e.g., *Storey and Zeippen*, 2000, equation (4)] incorporating relativistic effects, that were not utilized in the calculations mentioned above, may serve to increase the magnitude of the O(^{1}S − ^{3}P) transition probability. Such corrections have been shown to impact the intensity ratios of other optically forbidden transitions proceeding by magnetic dipole radiation that are observed in the nightglow, such as N(^{2}D − ^{4}S) 519.8/520.0 nm [*Butler and Zeippen*, 1984] and O(^{1}S − ^{3}P) 630.0/636.4 nm [*Storey and Zeippen*, 2000].

3.2. Planetary Observations

[54] The spectrometers on planetary orbiters are typically designed to measure the UV spectral region to the exclusion of the visible. As a result, it is only the 297.2 nm line that is observed. Only the Venera 9/10 orbiters could measure the 557.7 nm line, and no such emission was seen, with an upper limit of 10 R.

[55] Subsequently, an apparent signal was seen in the Pioneer Venus data at 297.2 nm [*Huestis and Slanger*, 1993], but its intensity of ∼40 R implied a green line intensity of 800 Rayleighs when a ratio of $\mathcal{R}$ = 20 was adopted, a value based on the average of the theoretical and laboratory investigations. Such a high intensity was of course quite incompatible with the negative results from Venera 9/10. However, with a value of $\mathcal{R}$ = 9.8, the deduced 557.7 nm intensity becomes 390 Rayleighs, and in the meantime a measured Venus nightglow green line intensity of 170 Rayleighs has been reported [*Slanger et al.*, 2001a; *Slanger et al.*, 2006]. Thus instead of concluding that the 297.2 nm signal from Pioneer Venus was an artifact, it may represent the first O(^{1}S) detection in the Venus nightglow.

[56] O(^{1}S) dayglow at Venus is expected to be much more intense than on Mars, based on the solar geometric factor. The Mariner orbiters measured the 297.2 nm dayglow at Mars, finding slant intensities of 20 kR at limb crossings [*Barth et al.*, 1971]. Pioneer Venus measured the dayglow [*LeCompte et al.*, 1989], and reported nadir intensities on

the order of 7 kR. The Mars Express orbiter has identified UV nightglow at 190–250 nm originating with N + O recombination into the NO γ- and δ-band systems [*Bertaux et al.*, 2005], analogous to the Pioneer Venus results [*Stewart et al.*, 1979] and also to the 190–250 nm nightglow emission in the terrestrial atmosphere [*Eastes et al.*, 1992]. The data so far processed show ambiguous results for 297.2 nm emission, but it is important to continue data collection, as the above discussion emphasizes that at Venus, the green line intensity shows great variability. The Venus Express mission that went into orbit in April 2006 has the same UV capability as Mars Express and will presumably record 297.2 nm signals and their variability in the nightglow and large signals in the dayglow.

[57] Another look at the Venus airglow will also be provided in June 2007, when the Messenger mission to Mercury performs a flyby of Venus (http://messenger.jhuapl.edu). The spectrometer on this probe will detect both UV and visible emission, and for the first time on a Venus/Mars mission both O(^{1}S) lines will be simultaneously observed. Hopefully the emissions will be in an intense phase of their variability cycle so that good comparisons can be made between the apparent $\mathcal{R}$ and the absolute value from the present study. In principle, all space missions in which there are simultaneous measurements of the two O(^{1}S) lines should confirm their UV/visible intensity calibration by this method.

4. Conclusions

[58] Owing to the significant differences that have existed between various theoretical and experimental determinations of $\mathcal{R}$, this branching ratio has been poorly known. In the present study a broad array of field observations, spanning 4 decades of investigations, has been analyzed and a very consistent branching ratio has resulted, with a value of 9.8 ± 1.0. This is well below most theoretical and experimental determinations, and makes the 297.2 nm line a more attractive target for O(^{1}S) studies than heretofore believed. It seems likely that for theoretical calculations, the strength of the O(^{1}S − ^{3}P) transition has been underestimated, while the most vulnerable part of the laboratory studies designed to measure the branching ratio is intensity calibration. Because the ratio is invariant in low-pressure systems, it can be considered a standard for measurements connecting the UV to the visible spectral regions.

[59] **Acknowledgments.** This study was supported by a grant from the NSF CEDAR program of the Aeronomy Division, ATM-0437361. We are grateful to Lyle Broadfoot for providing a value for $\mathcal{R}$ from GLO dayglow data and to Jerry Owens for providing spectra from the ISO/ATLAS-1 mission. Analysis of the ISAAC data was supported by the Office of Naval Research, grant N00014031073.

[60] Wolfgang Baumjohann thanks Alexander Dalgarno and another reviewer for their assistance in evaluating this paper.

References

Ångstrom, A. J. (1869), Spectrum des Nordlichts, *Pogg. Ann.*, *137*, 161–163.

Baluja, K. L., and C. J. Zeippen (1988), M1 and E2 transition probabilities for states within the $2p^2$ configuration of the OI isoelectronic sequence, *J. Phys. B*, *21*, 1455–1471.

Barth, C. A., C. W. Hord, J. B. Pearce, K. K. Kelly, G. P. Anderson, and A. I. Stewart (1971), Mariner 6 and 7 ultraviolet spectrometer experiment: Upper atmosphere data, *J. Geophys. Res.*, *76*, 2213–2227.

Bates, D. R. (1989), Oxygen band system transition arrays, *Planet. Space Sci.*, *37*, 811–817.

Bertaux, J.-L., et al. (2005), Nightglow in the upper atmosphere of Mars and implications for atmospheric transport, *Science*, *307*, 566–569.

Black, G., R. L. Sharpless, and T. G. Slanger (1975), Collision-induced emission from O(^{1}S) by He, Ar, N_2, H_2, Kr, and Xe, *J. Chem. Phys.*, *63*, 4546–4550.

Broadfoot, A. L., D. B. Hatfield, E. R. Anderson, T. C. Stone, B. R. Sandel, J. A. Gardner, E. Murad, D. J. Knecht, C. P. Pike, and R. A. Viereck (1997), N_2 triplet band systems and atomic oxygen in the dayglow, *J. Geophys. Res.*, *102*, 11,567–11,584.

Butler, K., and C. J. Zeippen (1984), N I forbidden lines revisited, *Astron. Astrophys.*, *141*, 274–278.

Condon, E. U. (1934), The absolute intensity of the nebular lines, *Astrophys. J.*, *79*, 217–234.

Cosby, P. C., B. D. Sharpee, D. L. Huestis, T. G. Slanger, and R. Hanuschik (2006), High-resolution terrestrial nightglow emission line atlas from UVES/VLT: Positions, intensities, and assignments for 2808 lines at 314–1043 nm, *J. Geophys. Res.*, *111*, A12307, doi:10.1029/2006JA012023.

Cunningham, D. L., and K. C. Clark (1974), Rates of collision-induced emission from metastable O(^{1}S) atoms, *J. Chem. Phys.*, *61*, 1118–1124.

Degen, V. (1972), Excitation of the Herzberg bands of O_2 in laboratory afterglow and night airglow, *J. Geophys. Res.*, *27*, 6213–6218.

Degen, V. (1977), Nightglow emission rates in the O_2 Herzberg bands, *J. Geophys. Res.*, *82*, 2437–2438.

Eastes, R. W., R. E. Huffman, and F. J. LeBlanc (1992), NO and O_2 ultraviolet nightglow and spacecraft glow from the *S3-4* satellite, *Planet. Space Sci.*, *40*, 481–493.

Fateev, A. A., V. S. Ivanov, A. M. Pravilov, and L. G. Smirnova (1996), Relative Einstein coefficients and dipole moments of the $O_2(A^3\Sigma_u^+, v' - X^3\Sigma_g^-, v''; c^1\Sigma_u^-, v' - X^3\Sigma_g^-, v'')$ transitions measured in oxygen atom recombination accompanied by radiation, *J. Phys. B*, *29*, 1351–1467.

Fischer, C. F., and H. Saha (1983), Multiconfiguration Hartree-Fock results with Breit-Pauli corrections for forbidden transitions in the 2p(4) configuration, *Phys. Rev. A*, *28*, 3169–3178.

Fischer, C. F., and G. Tachiev (2004), Breit-Pauli energy levels, lifetimes, and transition probabilities for beryllium-like and neon-like sequences, *At. Data Nucl. Data Tables*, *87*, 1–184.

Galavis, M. E., C. Mendoza, and C. J. Zeippen (1997), Atomic data from the Iron Project. XXII. Radiative rates for forbidden transitions within the ground configuration of ions in the carbon and oxygen isoelectronic sequences, *Astron. Astrophys. Suppl. Ser.*, *123*, 159–171.

Garstang, R. H. (1951), Energy levels and transition probabilities in p^2 and p^4 configurations, *Mon. Not. R. Astron. Soc.*, *111*, 115.

Garstang, R. H. (1955), Transition probabilities of auroral lines, in *The Airglow and the Aurora*, edited by E. B. Armstrong and A. Dalgarno, p. 324, Elsevier, New York.

Greer, R. G. H., et al. (1986), ETON 1: A data base pertinent to the study of energy transfer in the oxygen nightglow, *Planet. Space Sci.*, *34*, 771–788.

Hanuschik, R. W. (2003), A flux-calibrated high-resolution atlas of optical sky emission from UVES, *Astron. Astrophys.*, *407*, 1157–1164.

Hennes, J. P. (1966), Measurement of the ultraviolet nightglow spectrum, *J. Geophys. Res.*, *71*, 763–770.

Hill, S. M., S. C. Solomon, D. D. Cleary, and A. L. Broadfoot (2000), Temperature dependence of the reaction $N_2(A^3\Sigma_u^+)$ + O in the terrestrial thermosphere, *J. Geophys. Res.*, *105*, 10,615–10,629.

Huestis, D. L., and T. G. Slanger (1993), New perspectives on the Venus nightglow, *J. Geophys. Res.*, *98*, 10,839–10,847.

Kernahan, J. A., and P. H.-L. Pang (1975), Experimental determination of absolute A coefficients for "forbidden" atomic oxygen lines, *Can. J. Phys.*, *53*, 455–458.

Klotz, R., and S. D. Peyerimhoff (1986), Theoretical study of the intensity of the spin- or dipole forbidden transitions between the $c^1\Sigma_u^-$, $A'^3\Delta_u$, $A^3\Sigma_u^+$ and $X^3\Sigma_g^-$, $a^1\Delta_g$, $b^1\Sigma_g^+$ states in O_2, *Molec. Phys.*, *57*, 573–594.

LeBlanc, F. J., G. Oldenberg, and N. P. Carleton (1966), Transition probabilities of forbidden oxygen lines in a discharge tube, *J. Chem. Phys.*, *45*, 2200–2203.

LeCompte, M. A., L. J. Paxton, and A. I. F. Stewart (1989), Analysis and interpretation of observations of airglow at 297 nm in the Venus thermosphere, *J. Geophys. Res.*, *94*, 208–216.

McConkey, J. W., D. J. Burns, K. A. Moran, and K. G. Emeleus (1966), Measurement of relative multipole transition probabilities in atomic oxygen, *Phys. Lett.*, *22*, 416–417.

Melo, S. M. L., H. Takahashi, B. R. Clemesha, and J. Stegman (1997), The O_2 Herzberg I bands in the equatorial nightglow, *J. Atmos. Sol. Terr. Phys.*, *59*, 295–303.

Minschwaner, K., J. Bishop, S. A. Budzien, K. F. Dymond, D. E. Siskind, M. H. Stevens, and R. P. McCoy (2004), Middle and upper thermospheric odd nitrogen: 2. Measurements of nitric oxide from Ionospheric Spectro-

scopy and Atmospheric Chemistry (ISAAC) satellite observations of NO γ band emission, *J. Geophys. Res.*, *109*, A01304, doi:10.1029/2003JA009941.

Murtagh, D. R., I. C. McDade, R. G. H. Greer, J. Stegman, G. Witt, and E. J. Llewellyn (1986), ETON 4: An experimental investigation of the altitude dependence of the $O_2(A^3\Sigma_u^+)$ vibrational populations in the nightglow, *Planet. Space Sci.*, *34*, 811–817.

Nicolaides, C., O. Sinanoglu, and P. Westhaus (1971), Theory of atomic structure including electron correlation. IV. Method for forbidden-transition probabilities with results for [OI], [OII], [OIII], [NI], [NII], and [CI], *Phys. Rev. A*, *4*, 1400–1410.

Ogawa, T., N. Iwagami, M. Nakamura, M. Takano, H. Tanabe, A. Takechi, A. Miyashita, and K. Suzuki (1987), A simultaneous observation of the height profiles of the night airglow OI 5577 Å, O_2 Herzberg and atmospheric bands, *J. Geomagn. Geoelectr.*, *39*, 211–228.

Owens, J. K., et al. (1993), Mesospheric nightglow spectral survey taken by the ISO Spectral Spatial Imager on Atlas 1, *Geophys. Res. Lett.*, *20*, 515–518.

Pasternack, S. (1940), Transition probabilities of forbidden lines, *Astrophys. J.*, *92*, 126.

Petrignani, A., F. Hellberg, R. D. Thomas, M. Larsson, P. C. Cosby, and W. J. v. d. Zande (2005), Electron energy-dependent product state distributions in the dissociative recombination of O_2^+, *J. Chem. Phys.*, *122*, 234–311.

Santoro, A. L., D. L. Huestis, and T. G. Slanger (1994), Spectral analysis of Atlas I/ISO O_2 ultraviolet nightglow data, and comparison with laboratory afterglows, *Eos Trans. AGU*, *75*(44), Fall Meet. Suppl., F496.

Sharp, W. E., and D. E. Siskind (1989), Atomic emission in the ultraviolet nightglow, *Geophys. Res. Lett.*, *16*, 1453–1456.

Sharpee, B. D., and T. G. Slanger (2006), The O(^{1}D$_2$-^{3}P$_{2,1,0}$) 630.0, 636.4, and 639.2 nm forbidden emission line intensity ratios measured in the terrestrial nightglow, *J. Phys. Chem. A*, *110*(21), doi:10.1021/jp056163x.

Sharpee, B. D., T. G. Slanger, P. C. Cosby, and D. L. Huestis (2005), The N(^{2}D°-^{4}S°) 520 nm forbidden doublet in the nightglow: An experimental test of the theoretical intensity ratio, *Geophys. Res. Lett.*, *32*, L12106, doi:10.1029/2005GL023044.

Slanger, T. G., and R. A. Copeland (2003), Energetic oxygen in the upper atmosphere and the laboratory, *Chem. Rev.*, *103*(12), 4731–4765.

Slanger, T. G., and D. L. Huestis (1983), The rotationally resolved 3400- to 3800 A terrestrial nightglow, *J. Geophys. Res.*, *88*, 4137–4139.

Slanger, T. G., and D. E. Osterbrock (2000), Investigation of potassium, lithium, and sodium emissions in the nightglow, and OH cross-calibration, *J. Geophys. Res.*, *105*, 1425–1429.

Slanger, T. G., P. C. Cosby, D. L. Huestis, and D. E. Osterbrock (2000a), Vibrational level distribution of $O_2(b^1\Sigma_g^+$, v = 0–15) in the mesosphere and lower thermosphere region, *J. Geophys. Res.*, *105*, 20,557–20,564.

Slanger, T. G., D. L. Huestis, P. C. Cosby, and D. E. Osterbrock (2000b), Accurate atomic line wavelengths from astronomical sky spectra, *J. Chem. Phys.*, *113*, 8514–8520.

Slanger, T. G., P. C. Cosby, D. L. Huestis, and T. A. Bida (2001a), Discovery of the atomic oxygen green line in the Venus night airglow, *Science*, *291*, 463–465.

Slanger, T. G., D. L. Huestis, P. C. Cosby, and T. A. Bida (2001b), Nightglow studies with the world's largest optical telescope, *Adv. Space Res.*, *27*, 1135–1145.

Slanger, T. G., P. C. Cosby, and D. L. Huestis (2003a), Ground-based observation of high-altitude high-temperature emission in the O_2 atmospheric band nightglow, *J. Geophys. Res.*, *108*(A7), 1293, doi:10.1029/2003JA009885.

Slanger, T. G., P. C. Cosby, and D. L. Huestis (2003b), A new O_2 band system: The $c^1\Sigma_u^- - b^1\Sigma_g^+$ transition in the terrestrial nightglow, *J. Geophys. Res.*, *108*(A2), 1089, doi:10.1029/2002JA009677.

Slanger, T. G., P. C. Cosby, D. L. Huestis, and A. M. Widhalm (2004a), Nightglow vibrational distributions in the *A* and *A′* states of O_2 derived from astronomical sky spectra, *Ann. Geophys.*, *22*, 3305–3314.

Slanger, T. G., D. L. Huestis, P. C. Cosby, and R. R. Meier (2004b), Oxygen atom Rydberg emission in the equatorial ionosphere from radiative recombination, *J. Geophys. Res.*, *109*, A10309, doi:10.1029/2004JA010556.

Slanger, T. G., D. L. Huestis, P. C. Cosby, N. J. Chanover, and T. A. Bida (2006), The Venus nightglow: Ground-based observations and chemical mechanisms, *Icarus*, *182*, 1–9.

Stegman, J., and D. P. Murtagh (1988), High resolution spectroscopy of oxygen UV airglow, *Planet. Space Sci.*, *36*, 927–934.

Stegman, J., and D. P. Murtagh (1991), The molecular oxygen band systems in the UV nightglow: Measured and modelled, *Planet. Space Sci.*, *39*, 595–609.

Stewart, A. I., J. D. E. Anderson, L. W. Esposito, and C. A. Barth (1979), Ultraviolet spectroscopy of Venus: Initial results from the Pioneer Venus Orbiter, *Science*, *203*, 777.

Storey, P. J., and C. P. Zeippen (2000), Theoretical values for the [OIII] 5007/4959 line-intensity ratio and homologous cases, *Mon. Not. R. Astron. Soc.*, *312*, 813–816.

Thomas, R. J., and R. A. Young (1981), Measurement of atomic oxygen and related airglows in the lower thermosphere, *J. Geophys. Res.*, *86*, 7389.

Thomas, L., R. G. H. Greer, and P. H. G. Dickinson (1979), The excitation of the 557.7 nm lines and Herzberg bands in the nightglow, *Planet. Space Sci.*, *27*, 925–931.

Torr, D. G., M. R. Torr, and P. G. Richards (1993), Thermospheric airglow emissions: A comparison of measurements from ATLAS-1 and theory, *Geophys. Res. Lett.*, *20*, 519–522.

Wiese, W. L., J. R. Fuhr, and T. M. Deters (Eds.) (1996), *Atomic Transition Probabilities of Carbon, Nitrogen, and Oxygen: A Critical Data Compilation*, Am. Chem. Soc., Washington, D. C.

Wolfram, K. D., K. F. Dymond, S. A. Budzien, C. P. Fortna, R. P. McCoy, and E. J. Bucsela (1999), The Ionospheric Spectroscopy and Atmospheric Chemistry experiment on the Advanced Research and Global Observing Satellite: Quick look results, in *Ultraviolet Atmospheric and Space Remote Sensing: Methods and Instrumentation*, vol. II, edited by G. P. Carruthers and J. F. Dymond, pp. 149–159, Int. Soc. for Opt. Eng., Bellingham, Wash.

Yamanouchi, T., and H. Horie (1952), Intensities of forbidden lines of atoms in pn configurations, *J. Phys. Soc. Jpn.*, *7*, 52–57.

P. C. Cosby, B. D. Sharpee, and T. G. Slanger, Molecular Physics Laboratory, SRI International, Menlo Park, CA 94025, USA. (tom.slanger@sri.com)

K. R. Minschwaner, New Mexico Institute of Mining and Technology, Socorro, NM 87801, USA.

D. E. Siskind, Naval Research Laboratory, Washington, DC 20376, USA.